LAWRENCE
LIVERMORE
NATIONAL
LABORATORY

LLNL-PROC-636392

Compton scattering gamma-ray light source modeling and optimization

S. S. Q. Wu, R. A. Marsh, F. V. Hartemann

May 10, 2013

Compton scattering gamma-ray light source modeling and optimization
Shanghai, China
May 12, 2013 through May 17, 2013

Disclaimer

COMPTON SCATTERING GAMMA-RAY LIGHT SOURCE MODELING AND OPTIMIZATION*

S.S.Q. Wu, R.A. Marsh, F.V. Hartemann†, LLNL, CA 94550, USA

Abstract

In Compton scattering light sources, a short (ps to ns) laser pulse and a high brightness relativistic electron beam collide to yield tunable, monochromatic, polarized gamma-ray photons. The properties of the gamma-ray phase space is studied, in relation to the full electron bunch and laser pulse phase spaces, along with collimation, nonlinear effects and other sources of spectral broadening. This process has potential high impact applications in homeland security, nuclear waste assay, medical imaging and stockpile surveillance, among other areas of interest. Detailed theoretical modeling is outlined to aid the design of Compton light sources and provide optimization strategies relevant within the context of nuclear photonics applications.

INTRODUCTION

In Compton scattering light sources, a laser pulse is scattered by a relativistic electron beam to generate tunable radiation. Because of the inhomogeneous nature of the incident radiation, the relativistic Lorentz boost of the electrons is modulated by the ponderomotive force during the interaction, leading to intrinsic spectral broadening and brightness limitations. These effects are outlined, along with an optimization strategy to properly balance the laser bandwidth, diffraction, and nonlinear ponderomotive force.

PONDEROMOTIVE DEPHASING

QED units are used throughout: length, mass, time, and charge are measured in units of $\lambda\!\!\!^{-}=\hbar/m_0c$, m_0, $\lambda\!\!\!^{-}/c$, and e, respectively. In these units, the permittivity of vacuum is $\varepsilon_0=1/4\pi\alpha$. We consider a relativistic electron interacting with a polychromatic plane wave described by the 4-potential: $A_\mu=\sigma_\mu A(\phi)$; $\phi=k_\mu x^\mu$, $\sigma_\mu\sigma^\mu=-1$. In the Lorentz gauge, $\partial_\mu A^\mu=0=k_\mu\sigma^\mu A'(\phi)$; and the Lorentz force equation can be solved exactly to obtain the electron nonlinear 4-velocity:

$$u_\mu=u_\mu^0+A_\mu-k_\mu\frac{A_\nu\left(A^\nu+2u_0^\nu\right)}{2k_\lambda u_0^\lambda}=u_\mu^0+\varepsilon_\mu A(\phi)+k_\mu\frac{A^2(\phi)}{2k_\lambda u_0^\lambda};$$

$$\varepsilon_\mu=\sigma_\mu-k_\mu\frac{\sigma_\nu u_0^\nu}{k_\lambda u_0^\lambda}.$$

In cases where the recoil parameter, $\mu=k_\mu q^\mu$, remains small, and spin effects can be ignored, the differential spectral brightness is adequately described by the classical radiation formula:

$$\frac{d^2N}{dqd\Omega}=\frac{\alpha q}{4\pi^2}\left|\pi^\mu\int_{-\infty}^{+\infty}u_\mu e^{iq_\nu x^\nu}\,d\tau\right|^2.$$

Here, q_μ is the scattered radiation 4-wavenumber; π_μ is its 4-polarization; and $x_\mu(\tau)$ is the electron 4-trajectory, parameterized by the proper time, τ.

For a plane wave of constant amplitude, $A(\phi)=A_0\cos\phi$, the electron 4-velocity is integrated to yield the 4-position:

$$x_\mu(\phi)=x_\mu^0+\int_0^\phi\frac{dx_\mu}{d\tau}\frac{d\tau}{d\varphi}d\varphi$$

$$=x_\mu^0+u_\mu^0\frac{\phi}{\kappa_0}+\varepsilon_\mu\frac{A_0}{\kappa_0}\sin\phi+k_\mu\frac{A_0^2}{8\kappa_0^2}(2\phi+\sin 2\phi).$$

$\kappa_0=k_\mu u_0^\mu=d\phi/d\tau$ is the incident light-cone variable and x_μ^0 is the initial 4-position. In the linear limit, where $A_0\ll 1$, the radiation integral can be approximated as:

$$\frac{\alpha qA_0^2}{4\pi^2\kappa^2}\left|\pi^\mu\int_{-\infty}^{+\infty}\left(\varepsilon_\mu\cos\phi-iu_\mu\frac{q_\nu\varepsilon^\nu}{\kappa}\sin\phi\right)e^{-iq_\nu\left(\frac{u^\nu}{\kappa}+k^\nu\frac{A_0^2}{4\kappa^2}\right)\phi}\,d\phi\right|^2.$$

Here, we have linearized the complex exponential; dropped the dc term; and neglected terms in A_0^2, except for the rectified 2nd harmonic in the radiation phase. For a square pulse, the integral is performed to yield:

$$\frac{\alpha qA_0^2\Delta\phi^2}{4\pi^2\kappa^2}\left|\left(\varepsilon_\mu\pm u_\mu\frac{q_\nu\varepsilon^\nu}{\kappa}\right)\mathrm{sinc}\left\{\Delta\phi\left[1\pm\left(\frac{\lambda}{\kappa}+\mu\frac{A_0^2}{4\kappa^2}\right)\right]\right\}\right|^2.$$

$\lambda=q_\mu u^\mu$ is the scattered light-cone variable and $\Delta\phi$ is the duration of the pulse. Focusing on the positive frequency sinc^2 spectrum, we note that the primary peak corresponds to a null argument, while the first zero is obtained when the argument is equal to π; we can then quantify the onset of significant ponderomotive dephasing as described in Fig. 1: starting from the linear case, where $A_0\to 0$, we find the Doppler shift condition, $\kappa-\lambda=0$; for a finite amplitude, the primary peak is downshifted,

and the first zero is located at $\frac{\Delta\phi}{\kappa}\left(\kappa-\lambda-\frac{\mu}{4\kappa}A_0^2\right)=\pi$. The ponderomotive dephasing onset is: $\frac{\mu}{4\kappa^2}A_0^2\Delta\phi=\pi$.

In the more general case of an arbitrary incident radiation pulse, the scattered radiation spectrum is proportional to:

$$\left|\pi^{\mu}\int_{-\infty}^{+\infty}\left[\varepsilon_{\mu}A(\phi)+iu_{\mu}\frac{q_{\nu}\varepsilon^{\nu}}{\kappa}\int_0^{\phi}A(\varphi)d\varphi\right]e^{i\left[\frac{\lambda}{\kappa}\phi+\frac{\mu}{2\kappa^2}\int_0^{\phi}\overline{A^2(\varphi)}d\varphi\right]}d\phi\right|^2.$$

The weakly nonlinear dephasing term, averaged over an optical cycle, plays an important role because it can result in a significant accumulated phase shift for sufficiently long pulses. In fact, this term is proportional to the total radiation probability: $N=\int\sigma j_{\mu}\Phi^{\mu}d^4x\simeq\frac{2}{3}\alpha\int_{-\infty}^{+\infty}\overline{A'^2}\,d\phi$.

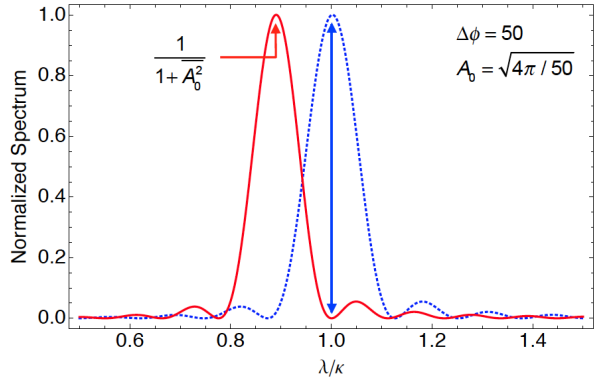

Fig. 1 Quadratic sinc spectra in the linear limit and with nonlinear dephasing.

THREE-DIMENSIONAL EFFECTS

We now address the fully three-dimensional case; working within the context of the paraxial approximation, for a linearly polarized, cylindrical Gaussian transverse distribution at focus, the transverse potential takes the form: $A_x=A_0g(\phi)e^{i\phi-\bar{r}^2(1-i\bar{z})^{-1}}(1-i\bar{z})^{-1}$. Here, $\phi=k_0(t+z)$ is the phase of the wave; $z_0=\frac{1}{2}k_0w_0^2$ is the Rayleigh length, expressed in terms of the focal waist, and axial wavenumber; $\bar{z}=z/z_0$; and $\bar{r}=r/w_0$. For an electron on-axis, the axial position as a function of phase is easily derived; using the rapidity, ρ the ballistic component is: $dz/d\phi=u_z/\kappa\simeq e^{-\rho}\sinh\rho/k_0$. The transverse potential driving the electron oscillation, measured along the ballistic initial electron trajectory can now be expressed as a function of phase.

For a synchronized reference electron; and in the ultra-relativistic case, where $e^{-\rho}\sinh\rho\simeq\frac{1}{2}$:

$$A_x\left[\bar{r}=0,z(\phi),\phi\right]\simeq A_0g(\phi)e^{i\phi}\left(1-i\frac{\phi}{k_0^2w_0^2}\right)^{-1}.$$

The pulse energy can be evaluated by integrating the Poynting vector flux through the focal plane over the pulse duration. Using $x=\phi/\Delta\phi$; and taking into account $|g'/g|\ll1$:

$$W_0\simeq\frac{A_0^2\Delta\phi k_0w_0^2}{16\alpha}\int_{-\infty}^{+\infty}g^2(x)dx=\overline{W}_0\int_{-\infty}^{+\infty}g^2(x)dx.$$

Since the maximum spectral density is radiated on-axis, we specialize our analysis to that situation, and for head-on collisions; the radiation phase is: $q_{\mu}x^{\mu}\simeq qe^{-2\rho}\phi/k_0=\chi\phi$.

The linear radiation integral reads:

$$S_0=\frac{4\alpha^2}{\pi^2}\overline{W}_0\eta^2\chi\left|\int_{-\infty}^{+\infty}\frac{g(x)}{1-i\eta^2x}e^{ix\Delta\phi(1-\chi)}dx\right|^2.$$

Here, we have introduced the normalized Doppler-shifted frequency, $\chi=qe^{-2\rho}/k_0$; the scale parameter $\eta=\sqrt{\Delta\phi}/k_0w_0$, which measures the balance between bandwidth and diffraction; and used the normalized incident pulse energy. For illustration, consider the case of a Gaussian temporal envelope, where the spectrum can be evaluated analytically. Rescaling the frequency as $\bar{\chi}=\frac{1}{\eta^2}+\frac{\Delta\phi}{2}(\chi-1)$, in the limit $\Delta\phi\to\infty$, we have:

$$S_0\simeq4\alpha^2\overline{W}_0\eta^{-2}e^{-2/\eta^4}e^{4\bar{\chi}/\eta^2}\Phi^2(\bar{\chi}).$$

The maximum value of the on-axis spectrum is obtained at $\bar{\chi}^*\lesssim1$; $f_{\Delta\phi}=S_0\left[\chi^*(\eta),\eta;\Delta\phi\right]/4\alpha^2\overline{W}_0$, is a strong function of η that also weakly depends on $\Delta\phi$, as illustrated in Fig. 2; the maximum is $f_{\infty}(\eta^*)\simeq3.15379$ at $\eta^*\simeq1.71024$, and $\bar{\chi}^*(\eta^*)\simeq-0.389338$.

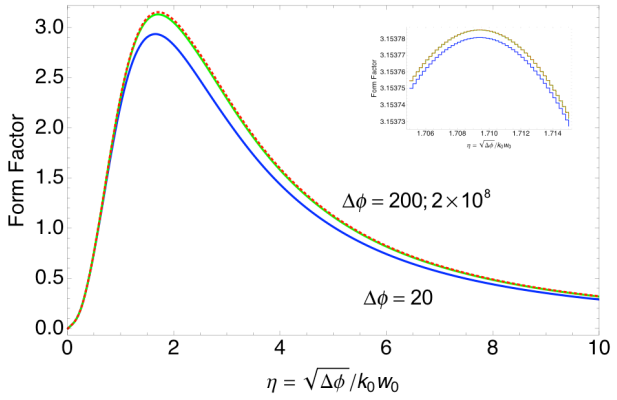

Fig. 2 Maximum angular and spectral brightness as function of η, for a fixed total energy, in the linear regime.

Physically, this is significant, as it shows that for a fixed incident laser pulse energy, the maximum number of photons scattered per unit solid angle and frequency is obtained when the transverse and axial scales are matched: $\sqrt{\Delta\phi} = \eta^* k_0 w_0$, which corresponds to a proper balance between bandwidth and diffraction. Furthermore, this condition is independent of the normalized potential: longer pulses diffracting slower will yield the same peak spectral density as long as the matching condition is satisfied: this approach is quite general.

For a self-consistent analysis, the effects of nonlinear dephasing are now included; the axial momentum is:

$$u_z(\bar{r}=0,\phi) \simeq \sinh\rho + \tfrac{k_0}{2\kappa} A_0^2 \left\{ \tfrac{1}{2} g e^{-i\phi} / \left[1 - i\bar{z}(\phi)\right] + \text{c.c.} \right\}.$$

The spectral density now reads:

$$\frac{\alpha}{16\pi^2} \frac{A_0^2 \Delta\phi^2}{k_0} \chi \left| \int_{-\infty}^{+\infty} \frac{g(x)}{1 - i\eta^2 x} e^{-ix\Delta\phi(1-\chi)} e^{i\chi \frac{A_0^2\Delta\phi}{2} \int_0^x \frac{g^2(y)}{1+\eta^4 y^2} dy} dx \right|^2 .$$

To study the interplay between bandwidth, diffraction, and weakly nonlinear effects, consider a Gaussian temporal envelope: $g(x) = e^{-x^2}$. We start from a linear spectrum with fixed bandwidth, $\Delta\phi^{-1}$; and matched in terms of diffraction: $\eta = \eta^*$. The ponderomotive dephasing, $\delta = A_0^2 \Delta\phi / 2$, is then varied to generate nonlinear spectra. This is equivalent to varying the incident pulse energy. For each spectrum, the maximum value of the main spectral line is determined, and plotted as a function of incident pulse energy on Fig. 3; for two different incident pulse durations corresponding to CPA (ps) and non-CPA (ns) laser technologies, respectively; and for three values of η.

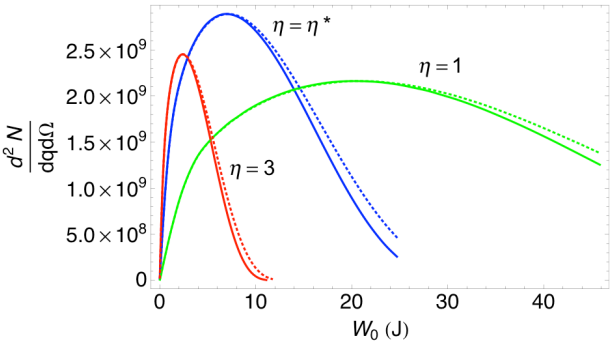

Fig. 3 Maximum brightness as a function of W_0 for $\Delta\phi = 10^3$ (dashed) and $\Delta\phi = 10^6$ (solid), and 3 values of η. The energy and brightness scales correspond to the long pulse; they have to be multiplied by 10^{-3} for the short pulse.

The (linear) matched beam produces the highest brightness, which scales very nearly linearly with the incident energy: higher energy allows one to use longer pulses and softer foci, which yield the best performance for our optimization metric. The most interesting conclusion is that the brightness degrades as one enters the nonlinear regime. Physically, this can be understood as follows: the nonlinear dephasing simply redistributes the scattered energy into parasitic channels, without increasing the main spectral line.

Finally, the maximum on-axis spectral and angular scattered photon number density, in units of photons per 0.1% bandwidth per mrad^2, for a balanced Gaussian-Lorentzian beam is determined as follows: we first define

$$B_x = \frac{d^2N}{dqd\Omega} \Delta q \Delta\Omega;$$

$$= \frac{\alpha}{4\pi^2} e^{2\rho} A_0^2 \Delta\phi^2 \chi^2 h(\eta, \Delta\phi, \chi, A_0) \times 10^{-9};$$

$$h = \left| \int_{-\infty}^{+\infty} \frac{e^{-x^2 - ix\Delta\phi(1-\chi)}}{1 - i\eta^2 x} e^{i\chi \frac{A_0^2\Delta\phi}{2} \int_0^x \frac{e^{-2y^2}}{1+\eta^4 y^2} dy} dx \right|^2 .$$

Here $\Delta q = q \times 10^{-3}$, and $\Delta\Omega = 10^{-6}$. Next, for a fixed value of $\Delta\phi$, the brightness triple maximum is found numerically:

$$B_x^* \simeq \tfrac{\alpha}{4\pi^2} A_0^{*2} \Delta\phi^2 e^{2\rho} \times 10^{-9} \times 0.241115 ;$$

with $\frac{A_0^{*2}\Delta\phi}{2} \int_{-\infty}^{+\infty} \frac{e^{-2x^2}}{1+\eta^{*4} x^2} dx = 2.704 \times 2\pi$. The incident pulse duration is $\Delta\phi / k_0$; the focal spot is $w_0 = \sqrt{\Delta\phi} / k_0 \eta^*$; and the energy is $W_0 = \sqrt{\tfrac{\pi}{2}} A_0^{*2} \Delta\phi^2 / \left(16\alpha k_0 \eta^{*2}\right)$.

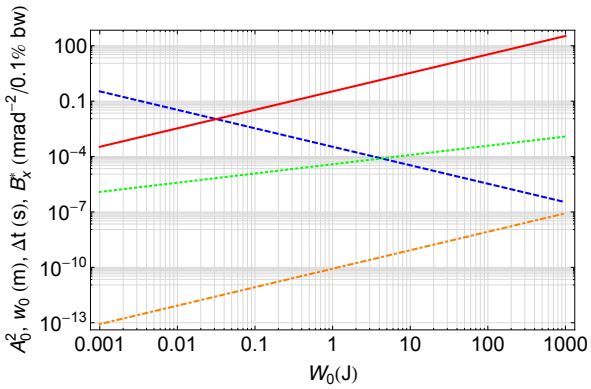

Fig. 4 Optimized nonlinear Gaussian-Lorentzian parameters as function of laser energy: A_0^{*2} (dashed); w_0 (dotted); Δt (dashed-dotted); and B_x^* (solid), for $\rho = 7.6$ ($\gamma = 10^3$).

* Work performed by LLNL for the US DoE under Contract # DE-AC52-07NA27344, & under LLNL 12ERD057

† hartemann1@llnl.gov